crystals

MDPI

Article

Effect on Compton Scattering Spectra by Hermite–Gaussian Light

Akane Agui [1,*], Hiroshi Sakurai [2], Naruki Tsuji [3], Haruka Ito [2] and Kiyofumi Nitta [3]

1 Synchrotron Radiation Research Center, Quantum Beam Science Research Directorate, National Institutes for Quantum and Radiological Science and Technology, Hyogo 679-5148, Japan
2 School of Science and Technology, Gunma University, Gunma 376-8515, Japan; sakuraih@gunma-u.ac.jp (H.S.); t191d009@gunma-u.ac.jp (H.I.)
3 Japan Synchrotron Radiation Research Institute, Hyogo 679-5198, Japan; ntsuji@spring8.or.jp (N.T.); nittak@spring8.or.jp (K.N.)
* Correspondence: agui.akane@qst.go.jp

Abstract: In this study, we measured the Compton scattering spectra of Al, Ag and Au metals changing the harmonic order of X-rays from an undulator. The width of the Compton scattered X-ray spectrum changed depending on the harmonic order of X-rays. This indicates that Compton scattering spectra shape reflects a momentum perpendicular to the traveling direction in Hermite–Gaussian (HG) light.

Keywords: Compton scattering; optical vortex; Hermite–Gaussian (HG) light; synchrotron radiation; undulator

Citation: Agui, A.; Sakurai, H.; Tsuji, N.; Ito, H.; Nitta, K. Effect on Compton Scattering Spectra by Hermite–Gaussian Light. *Crystals* **2021**, *11*, 650. https://doi.org/10.3390/cryst11060650

Academic Editor: Borislav Angelov

Received: 18 April 2021
Accepted: 3 June 2021
Published: 8 June 2021

1. Introduction

Since the establishment of electromagnetism at the end of the 19th century, it has been known that light generally has angular momentum, and that the spin angular momentum (helicity) of light corresponds to the polarized state. Allen pointed out that laser light with a Laguerre–Gaussian (LG) mode, which possesses a helicoidal wave-front surface around the propagation axis, has an orbital angular momentum [1]. Furthermore, it has been discovered that a phenomenon in which the light with an LG mode gives a rotational motion to an object [2]. This LG light is associated with the orbital angular momentum of light. After this discovery, it has been considered that the angular momentum of light consists of the spin angular momentum and the orbital angular momentum.

The orbital angular momentum of light has already been widely studied in laser physics. The orbital angular momentum of the LG wave function represented in the cylindrical coordinate system is a quantum number of this light.

The Hermite-Gaussian (HG) light is associated with the Cartesian coordinate system, and is in a conjugate relationship with the LG light as a linear combination. Both HG light and LG light are characterized by having momentums perpendicular to their traveling direction [1].

The wave function of HG light in the Cartesian coordinate system shows that the "number of nodes" of light is a good quantum number, and the momentum perpendicular to the traveling direction of light is quantized. The LG light, which is often called optical vortex, has been studied in laser physics and in synchrotron radiation research, among others. Theoretical and experimental studies have reported that X-rays generated as synchrotron radiation would generate an optical vortex [3–5]. Sasaki et al. reported that the synchrotron radiation with a circularly polarized component from the undulator has an optical vortex represented by LG light, and the linearly polarized light from the undulator has a "node" represented by HG light [6].

Recently, Nairat et al. showed that the initial angular momentum carried by the incident photon beam transfers to the scattered beam in Compton scattering process from the energy–momentum conservation laws [7]. Furthermore, Maruyama et al. reported theoretical calculations of a Compton scattered X-ray spectrum with LG and HG light, and pointed out that the Compton scattered X-ray spectrum depends on the number of nodes of HG light, which reflects the momentum perpendicular to the traveling direction of the quantized light [8,9].

In this study, we measure Compton scattered X-ray spectra to detect the momentum perpendicular to the traveling direction, which reflect the number of nodes of HG light of an undulator.

2. Compton Scattering between X-rays and Electrons

If we consider Compton scattering between X-rays and electrons, we get the following equations from the momentum conservation and energy conservation.

$$\mathbf{p} + \hbar\mathbf{k} = \mathbf{p}' + \hbar\mathbf{k}' \tag{1}$$

$$\frac{|\mathbf{p}|^2}{2m} + \hbar\omega = \frac{|\mathbf{p}'|^2}{2m} + \hbar\omega' \tag{2}$$

where $\mathbf{p}$ denotes an electron momentum in a material. $\mathbf{p'}$ denotes a momentum of a recoiled electron. $\hbar\mathbf{k}$ and $\hbar\omega$ denote an incident photon momentum and energy. $\hbar\mathbf{k'}$ and $\hbar\omega'$ denote a scattered photon momentum and energy. From Equations (1) and (2), we get

$$\hbar\omega' = \hbar\omega - \frac{\hbar^2|\mathbf{K}|^2}{2m} + \frac{\hbar\mathbf{pK}}{m} \tag{3}$$

where $\mathbf{K} = \mathbf{k} - \mathbf{k'}$. If we consider momenta of electrons, $\mathbf{p_1} = (p_{1x}, p_{1y}, p_{1z})$ and $\mathbf{p_2} = (p_{2x}, p_{2y}, p_{2z})$, in a material, we get

$$\hbar\omega'_1 = \hbar\omega - \frac{\hbar^2|\mathbf{K}|^2}{2m} - \frac{\hbar\mathbf{p}_1\mathbf{K}}{m} \text{ and } \hbar\omega'_2 = \hbar\omega - \frac{\hbar^2|\mathbf{K}|^2}{2m} - \frac{\hbar\mathbf{p}_2\mathbf{K}}{m} \tag{4}$$

Therefore

$$\hbar(\omega'_1 - \omega'_2) = \frac{\hbar(\mathbf{p}_2 - \mathbf{p}_1)\mathbf{K}}{m} \tag{5}$$

From Equation (5), we can understand that the full width of half maximum (FWHM) of the observed Compton scattered X-ray spectrum is therefore proportional to the FWHM of the electron momentum distribution of the material.

If we consider that the HG light has the momentum perpendicular to the traveling direction of the quantized light, $\mathbf{\Delta k}$, $\hbar\mathbf{k}$ in Equation (1) can be replaced by $\hbar$ ($\mathbf{k}$ + $\mathbf{\Delta k}$). Therefore Equation (5) for the HG light can be expressed by

$$\hbar(\omega'_{1HG} - \omega'_{2HG}) = \frac{\hbar(\mathbf{p}_2 - \mathbf{p}_1)(\mathbf{K} + \mathbf{\Delta k})}{m} \tag{6}$$

$$\frac{\hbar(\omega'_{1HG} - \omega'_{2HG})}{\hbar(\omega'_1 - \omega'_2)} = \frac{(\mathbf{p}_2 - \mathbf{p}_1)(\mathbf{K} + \mathbf{\Delta k})}{(\mathbf{p}_2 - \mathbf{p}_1)\mathbf{K}} = 1 + \frac{(\mathbf{p}_2 - \mathbf{p}_1)\mathbf{\Delta k}}{(\mathbf{p}_2 - \mathbf{p}_1)\mathbf{K}} \tag{7}$$

For the scattering angle of 90° with the scattering plane perpendicular to the linear polarization vector, as discussed in Materials and Methods later, $\mathbf{\Delta k}$ is perpendicular to $\mathbf{K}$. If we choose the *z*-axis along to $\mathbf{K}$ in momentum space, Equation (7) can be expressed by

$$\frac{\hbar(\omega'_{1HG} - \omega'_{2HG})}{\hbar(\omega'_1 - \omega'_2)} = \frac{(\mathbf{p}_2 - \mathbf{p}_1)(\mathbf{K} + \mathbf{\Delta k})}{(\mathbf{p}_2 - \mathbf{p}_1)\mathbf{K}} = 1 + \frac{|\mathbf{\Delta k}|\left(p_{1\mathbf{x}\text{ or }\mathbf{y}} - p_{2\mathbf{x}\text{ or }\mathbf{y}}\right)}{|\mathbf{K}|(p_{1\mathbf{z}} - p_{2\mathbf{z}})} \tag{8}$$

For an isotropic material such as a polycrystal metal, Equation (8) becomes

$$\frac{\hbar(\omega'_{1HG} - \omega'_{2HG})}{\hbar(\omega'_1 - \omega'_2)} = \frac{(\mathbf{p}_2 - \mathbf{p}_1)(\mathbf{K} + \mathbf{\Delta k})}{(\mathbf{p}_2 - \mathbf{p}_1)\mathbf{K}} = 1 + \frac{|\mathbf{\Delta k}|}{|\mathbf{K}|} \tag{9}$$

Because we can regard as $|\mathbf{K}| \approx \sqrt{2}|\mathbf{k}|$ for the scattering angle of 90°, we can estimate the momentum perpendicular to the traveling direction in the HG light from the analysis of a full width at half maximum (FWHM) of a Compton scattered X-ray spectrum.

3. Materials and Methods

In this paper, we detect the spectral change of Compton scattered X-rays due to the momentum perpendicular to the traveling direction in the HG light. Measurements were performed on SPring-8 BL37XU [10] with linearly polarized X-rays emitted from the undulator with a polarization vector in the horizontal plane. Figure 1 shows observed X-ray intensities, which are monochromatized to 114 keV by a Si 333–Si 511 double crystal monochromator, with changing undulator gaps as an example. By changing the undulator gap, a HG mode with a given harmonics number was chosen. In the present experiment, we used X-rays with 18, 19, 20, or 21st harmonics number (order of light) of the undulator. The emitted X-rays were monochromatized to 100 keV (energy width $\Delta E/E = 2 \times 10^{-5}$) by a Si 333–Si 511 double crystal monochromator, and irradiated on the sample. The center part of the X-ray was selected by a slit (0.5 mm × 0.5 mm) at the front end (30 m from the light source point). Figure 2 shows the experimental layout. Compton scattered X-rays were detected by a Ge solid state detector with a scattering angle of 90°. The scattering plane was set perpendicular to the linear polarization vector in the present experiment (90°, geometry in Figure 2).

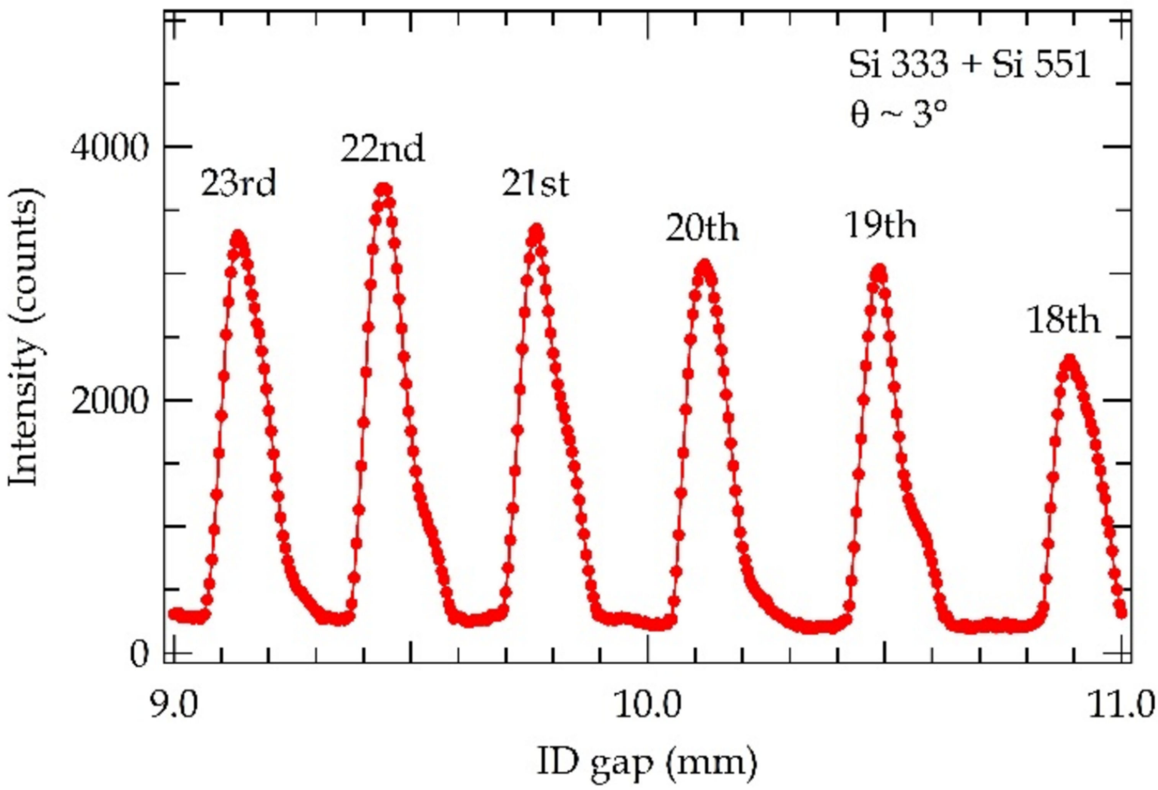

Figure 1. Observed X-ray intensities, which are monochromatized to 114 keV by a Si 333–Si 511 double crystal monochromator, with changing undulator gap. We can adjust the emission peak of a harmonics number of generated X-rays by tuning the undulator gap.

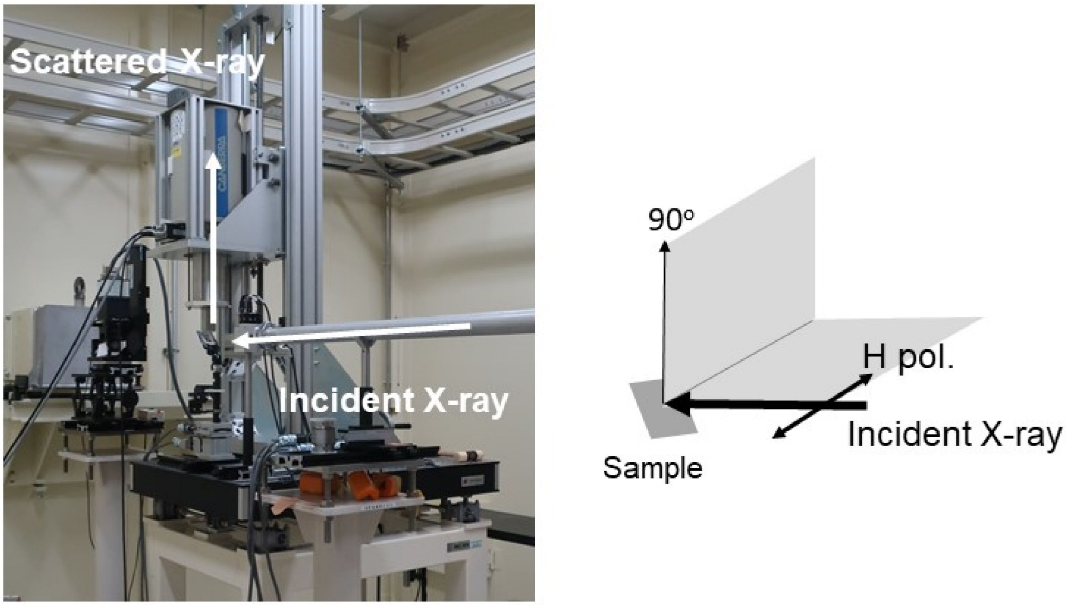

Figure 2. Experimental setup. Incident X-rays (come from the right) with horizontal polarization irradiates a sample. Scattered X-rays are detected with a scattering angle of 90°. The scattering plane is perpendicular to the linear polarization vector (H. pol.), which is shown as 90°.

Polycrystalline metals of Al, Ag and Au were measured as samples, because their electric state is described as a nearly free electron model and regarded as the isotropic electron momentum distribution system. The Compton scattering X-ray spectra were measured for Ag and Al with an 18, 19, 20, or 21st harmonic order, and Au with an 18 or 21st harmonic order of undulator. The measurements were performed at room temperature.

4. Results and Discussions

Figure 3a shows the Compton scattering spectra of Ag and Al samples for the incident X-ray with an 18, 19, 20, and 21st harmonic order of undulator. Although the spectral shapes depend on the sample clearly, dependences on the harmonic order of undulator are not clear, as shown in Figure 3a. Therefore, we performed analysis for the Compton scattered X-ray spectra by superimposing two Gaussian fittings. Figure 3b shows an example of fitting results for Al samples of the 21st harmonic order of the undulator. We call the broad FWHM, which corresponds to a momentum distribution of the core electrons, Width_1 (broad), and the narrower FWHM, which corresponds to a momentum distribution the valence electrons, Width_2 (narrow) [11]. Figure 4a shows the harmonic order dependence of Width_1 (broad) and Width_2 (narrow) for Al, Ag and Au. Here, we focus on Width_1 (broad) of Al and Width_2 (narrow) of Al, Ag and Au to avoid BG contributions such as lead fluorescence. The dependences on the harmonic order of undulator for Width_1 (broad) and Width_2 (narrow) are small. However, we seem to catch oscillations of Width_1 (broad) and Width_2 (narrow), as shown in Figure 4a.

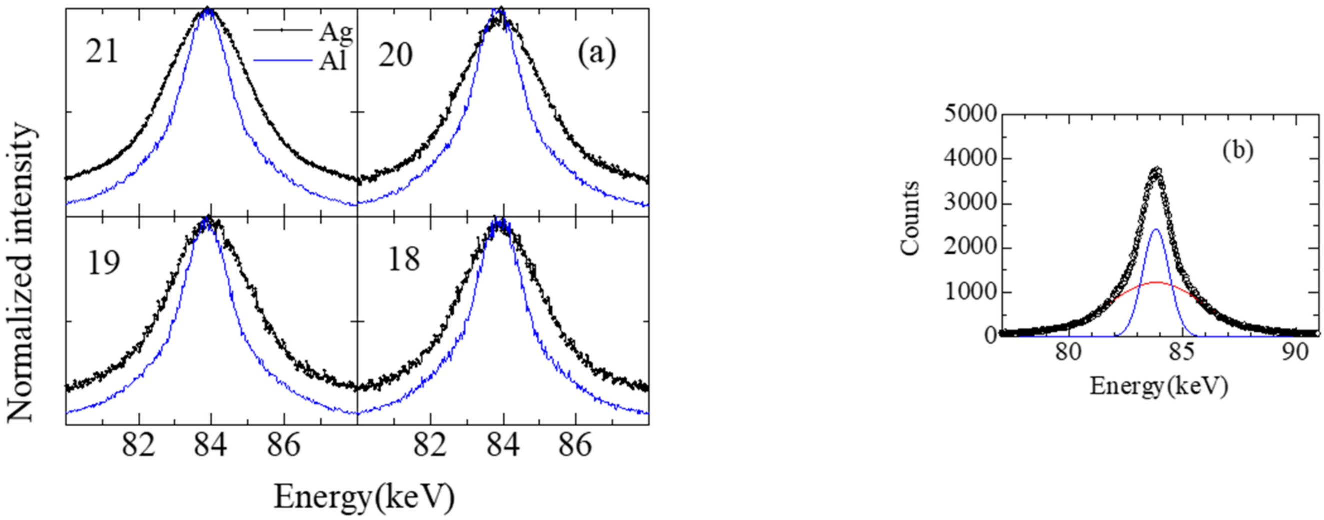

Figure 3. (**a**) Compton scattered spectra for Al and Ag. (**b**) An example of two Gaussian fitting of a Compton scattered X-ray spectrum for A1, 21st harmonic order of undulator. Circle: experimental, Red: Width_1 (Broad). Blue: Width_2 (Narrow). Bold: Fitting result (Width_1 + Width_2).

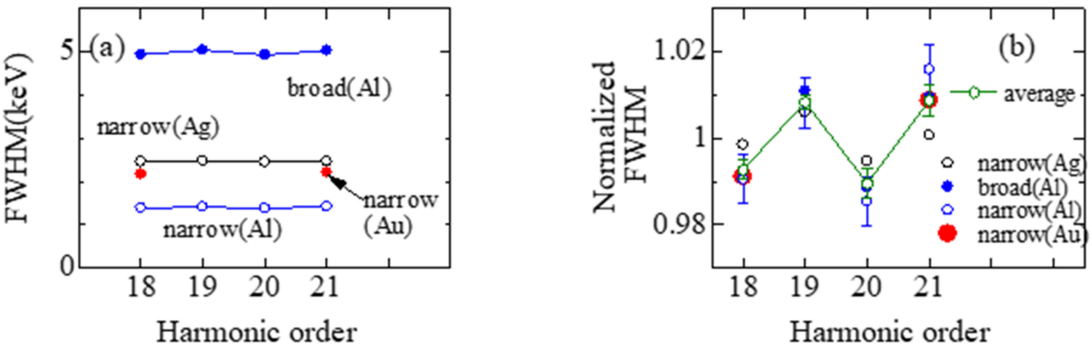

Figure 4. (**a**) Dependence on harmonic order of undulator for FWHMs of Compton scattering spectra (Width_1 (broad) and Width_2(narrow)). The estimated errors are about 0.6%, which is within the dot size (**b**) normalized values of the FWHMs in (**a**). The typical errors are shown for Width_2(narrow) of Al. The error of average is also shown.

In order to highlight the oscillations of the half-width, the half-widths are normalized by an average value among the four half-widths of harmonic orders of the undulator, as the following.

$$\text{Normalized Width\_}n = (\text{Width\_}n)/(\text{Width\_}n\text{\_Ave}) \quad (10)$$

where n = 1 or 2. Width_n_Ave denotes the average value of Width_n among the four half widths of harmonic orders of the undulator.

Figure 4b shows the Normalized Width_n obtained from Equation (10) for Al, Ag and Au. The oscillation behaviors of Normalized Width_n are observed in Figure 4b. The oscillation behaviors show that the normalized Width_n increases on the odd harmonic orders of the undulator, and decreases on the even harmonic orders of the undulator. This behavior may come from the difference in the node of HG light. The difference of Normalized Width_n between the odd and even order is about 0.01 (1%) on average. Since a momentum perpendicular to the traveling direction in the HG light is reflected by an FWHM of a Compton scattered X-ray spectrum, as discussed in Equation (10), the dependence on the harmonic orders of the undulator for the normalized Width_n can be ascribed to difference of the momentum perpendicular to the traveling direction in the HG light. The order of the value of momentum perpendicular to the traveling direction is estimated to be 1% of the momentum of the incident X-rays.

5. Conclusions

We measured Compton scattering spectra of simple metals, changing the harmonic orders of the undulator. The FWHM of Compton scattered X-ray spectrum depends on the harmonic order of the undulator. The order of the value of momentum perpendicular to the traveling direction is estimated to be 1% of the momentum of the incident X-rays.

This indicates Compton scattering spectra analysis is a candidate to study HG light in high energy X-ray regions.

Author Contributions: Writing, original draft preparation, A.A.; writing-review and editing, H.S.; Experimental design, N.T. and K.N., Data analysis, H.I., project administration, A.A.; funding acquisition, A.A. and H.S. All authors have read and agreed to the published version of the manuscript.

Funding: This research was funded by This work was supported by JSPS KAKENHI Grant Number 18K04952 and 19K04464.

Institutional Review Board Statement: Not applicable.

Informed Consent Statement: Not applicable.

Data Availability Statement: The data presented in this study are available on request from the corresponding author.

Acknowledgments: This work was supported by JSPS KAKENHI Grant Number 18K04952 and 19K04464. The synchrotron radiation experiments were performed at the BL08W and BL37XU of SPring-8 with the approval of the Japan Synchrotron Radiation Research Institute (JASRI) (Proposal No. 2019A1322 and 2019A1324).

Conflicts of Interest: The authors declare no conflict of interest.

References

1. Allen, L.; Beijersbergen, M.W.; Spreeuw, R.J.C.; Woerdman, J.P. Orbital Angular Momentum of Light and the Transformation of Laguerre-Gaussian Laser Modes. *Phys. Rev. A* **1992**, *45*, 8185. [CrossRef] [PubMed]
2. Friese, M.E.J.; Enger, J.; Rubinsztein-Dunlop, H.; Heckenberg, N.R. Optical angular-momentum transfer to trapped absorbing particles. *Phys. Rev. A* **1994**, *54*, 1593. [CrossRef]
3. Sasaki, S.; MNuly, I.; Dejus, R. Undulator radiation carrying spin and orbital angular momentum. *Nucl. Instrum. Meth. A* **2007**, *582*, 43. [CrossRef]
4. Katoh, M.; Fujimoto, M.; Kawaguchi, H.; Tsuchiya, K.; Ohmi, K.; Kaneyasu, T.; Taira, Y.; Hosaka, M.; Mochihashi, A.; Takasima, Y. Angular momentum of twisted radiation from an electron in spiral motion. *Phys. Rev. Lett.* **2017**, *118*, 094801. [CrossRef] [PubMed]
5. Katoh, M.; Fujimoto, M.; Mirian, N.S.; Konomi, T.; Taira, Y.; Kaneyasu, T.; Hosaka, M.; Yamamoto, N.; Moshihashi, A.; Takashima, Y. Helical phase structure of radiation from an electron in circular motion. *Sci. Rep.* **2017**, *7*, 6130. [CrossRef] [PubMed]
6. Sasaki, S.; McNuly, I. Proposal for generating brilliant x-ray beams carrying orbital angular momentum. *Phys. Rev. Lett.* **2008**, *100*, 124801. [CrossRef] [PubMed]
7. Nairat, M.; Goedecke, G.; Voelz, D. Compton Scattering of a Vortex Light Beam. *Bull. Am. Phys. Soc.* **2014**, *59*, 6. [CrossRef]
8. Maruyama, T.; Hayakawa, T.; Kajino, T. Compton Scattering of γ-Ray Vortex with Laguerre Gaussian Wave Function. *Sci. Rep.* **2019**, *9*, 51. [CrossRef] [PubMed]
9. Maruyama, T.; Hayakawa, T.; Kajino, T. Compton Scattering of Hermite Gaussian Wave γ Ray. *Sci. Rep.* **2019**, *9*, 7998. [CrossRef] [PubMed]
10. Terada, Y.; Tanida, H.; Uruga, T.; Takeuchi, A.; Suzuki, Y.; Goto, S. High-Resolution X-ray Microprobe Using a Spatial Filter and Its Application to Micro-XAFS Measurements. In Proceedings of the AIP Conference, Geneva, Switzerland, 15–20 September 2017; Volume 1365, pp. 172–175.
11. Cooper, M.J.; Cooper, M.; Mijnarends, P.E.; Mijnarends, P.; Shiotani, N.; Sakai, N.; Bansil, A. *X-ray Compton Scattering*; Oxford University Press: Oxford, UK, 2004.